research papers

Symmetry of single-wall nanotubes

M. Damnjanović,* T. Vuković, I. Milošević and B. Nikolić

Faculty of Physics, University of Belgrade, POB 368, Belgrade 11001, Yugoslavia. Correspondence e-mail: yqoq@afrodita.rcub.bg.ac.yu

Nanotubes have become attractive subjects in solid-state physics owing to their potential applications in nanotechnology. Their symmetry is one of the important tools in theoretical investigations. Here a review is presented of the symmetry groups of the single-wall nano- and microtubes considered in literature: BN, GaN, MS_2, C, BC_3, BC_2N.

1. Introduction

During the last decade, nanotubes have been among the most frequently studied physical systems. This interest stems from their amazing properties promising high applicability in future technology, *e.g.* variations in chirality and/or diameter of carbon nanotubes result in change, sometimes tremendous, of conductivity or optical properties, which enables fine tuning of the desired characteristics. From Iijima's first synthesis (Iijima, 1991) of carbon nanotubes, several other types of nanotube and microtube have been found: here different types of $B_xC_yN_z$, WS_2 and MoS_2 tubes are mentioned only.

A common characteristic of these compounds is their high symmetry, which has been revealed and applied in various calculations from the very beginning of research on carbon nanotubes. Their first classification was according to the principal axis of the parent C_{60} molecule (Dresselhaus *et al.*, 1992), which involved only part of the point-group symmetry; analyses of translational (Hamada *et al.*, 1992) and helical and rotational symmetries (White *et al.*, 1993; Jishi *et al.*, 1995; Saito *et al.*, 1998) in the context of electronic properties have been completed recently (Damnjanović *et al.*, 1999*a,b*) by inclusion of parities in the full symmetry group. On the contrary, the other tubes are less studied and almost no attempt in this direction has been made.

The aim of this paper is to determine the full symmetry groups of the known single-wall nanotubes. All of them are (as are the carbon ones) quasi-1D cylindrical structures, periodic along their axis and long enough for application of crystal physics techniques. Besides this translational symmetry, they possess a nontrivial rotational axis of high order. The origin of these symmetries becomes transparent if the nanotube is imagined as a layer rolled up into a cylinder. Then, the layer lattice translations become the rototranslations. When this 2D lattice is invariant under a nontrivial point group, some of these operations may remain the symmetries of the obtained tube and must also be included in the resulting line group.

The quasi-1D crystalline structure implies that the symmetry group of the nanotube is one of the line groups, which are defined as subgroups of the 3D Euclidean group assembling all the symmetries of monoperiodic systems. Therefore, the task is to recognise the line group corresponding to a given tube, and a brief reminder on the line groups necessary to accomplish it is given in §2. The problem is solved by analysis of diperiodic layer symmetries compatible with the folding procedure, as sketched in §3. After these general considerations, the actual tubes are discussed in the rest of the paper. Finally, the main manifestations of the revealed symmetries in the nanotube physics are commented on.

Note that these compounds, obtained from a single layer, are single-wall nanotubes. Their coaxial arrangements are called multiwall tubes and are beyond the scope of this article.

2. Line groups

Line (monoperiodic, rod) groups describe the spatial symmetries of the system periodic (with period a) along one, conveniently taken as the z axis, direction (Milošević & Damnjanović, 1993; Milošević *et al.*, 1996, 1997). Typical examples are stereoregular polymers, quasi-1D subsystems of crystals and the nanotubes.

A line group $\mathbf{L}$ contains elements $(P|t)$ (Koster–Seitz symbol) leaving the z axis invariant, thus restricting the point translational factor P and t respectively to axial point-group operations (Janssen, 1973) and translations along the z axis. In cylindrical coordinates, its action is $(P|t) : (\rho, \phi, z) \mapsto (\rho, \phi', z + t)$. Such a structure of elements implies that each line group is a (weak direct) product $\mathbf{L} = \mathbf{ZP}$ of one *axial point group* $\mathbf{P}$ and one infinite cyclic group $\mathbf{Z}$. The groups within each of the seven families $\mathbf{C}_n$, $\mathbf{S}_{2n}$, $\mathbf{C}_{nh}$, $\mathbf{C}_{nv}$, $\mathbf{D}_n$, $\mathbf{D}_{nd}$, $\mathbf{D}_{nh}$ of axial point groups differ in order $n = 1, 2, \ldots$ of the principal rotational axis. On the other hand, two types of *generalized translation* group $\mathbf{Z}$, screw-axis $\mathbf{T}_q^r$ [including the special case of pure translations $\mathbf{T}(a) = \mathbf{T}_1^0(a)$] and glide plane $\mathbf{T}_c$, are generated by the transformations $z_q^r = (C_q^r | \frac{n}{q} a)$ (z_0 for pure translations) and $z_v = (\sigma_v | \frac{a}{2})$, respectively. Absence of the crystallographic restrictions on the order of the principal axis results in an infinite number of line groups, and they are

classified within 13 families, characterized by a compatible choice of the generalized translations group type and the axial point-group family (Table 1).

To determine the full symmetry of a nanotube, both the factors $\mathbf{Z}$ and $\mathbf{P}$ are to be found. Since $\mathbf{C}_n$ is a subgroup of index 2 or 4 in any axial point group, each line group has the subgroup $\mathbf{L}^{(1)} = \mathbf{T}_q^r(a)\mathbf{C}_n$ [especially $\mathbf{L}^{(1)} = \mathbf{T}(a)\mathbf{C}_n$ whenever $\mathbf{Z} = \mathbf{T}_c$] of the same index, being the maximal first family subgroup in $\mathbf{L}$. When this group is determined, it remains to check for possible glide planes and parities (horizontal U axes, and vertical and horizontal mirror planes, σ_v and σ_h).

3. Folded up layer symmetry

In this section, we sketch how the symmetry of a nanotube is determined with the help of the symmetry of an unfolded diperiodic layer. Since the presently synthesized tubes may be studied on the basis of the hexagonal layers only, the method will be elaborated for such a case for clarity. As will be shown, this is essentially sufficient even for BC_2N tubes, which can be (more naturally, perhaps) studied by use of a rectangular layer lattice. Therefore, it is not surprising that some of the results are analogous to those derived for the carbon nanotubes. Nevertheless, the method can be easily generalized to accommodate any diperiodic symmetry.

The starting fact is that each symmetry operation of a nanotube corresponds to some symmetry operation of the layer. The symmetries of the layers themselves form a diperiodic group (Wood, 1964; Litvin & Wike, 1991; Milošević *et al.*, 1998). Besides the two-dimensional lattice translations, there may be present second-order screw axes, glide planes and point-group operations. Analogously to the line groups, these subperiodic groups may also be factorized into the (two-dimensional) generalized translational and axial point group. Still, the present derivation is facilitated by the fact that all the hexagonal diperiodic groups $\mathbf{Dg}65 - \mathbf{Dg}80$ are symmorphic. Thus, they are (semidirect) products of an axial crystallographic point group (with the principal axis of either third or sixth order) and the 2D translational group generated by the lattice vectors $\mathbf{a}_1$ and $\mathbf{a}_2$ of equal length a_0 making an angle of $\pi/3$ (Fig. 1).

To form a tube (n_1, n_2), this layer is rolled up so that the *chiral* vector $\mathbf{c} = n_1\mathbf{a}_1 + n_2\mathbf{a}_2$ ($n_1, n_2 \in \mathbb{Z}$) becomes a circle in the perpendicular cross section of the tube. Obviously, the 2D lattice translations along the chiral vector form pure rotational symmetries $\mathbf{C}_n$ of the tube, generated by the minimal among them, C_n, where[1]

$$n = \mathrm{GCD}(n_1, n_2) \tag{1a}$$

(the greatest common divisor). On the other hand, the 2D lattice translations perpendicular to the chiral vector remain pure translational symmetries of the tube, generated by the

minimal one, $\mathbf{a} = -[(2n_2 + n_1)/n\mathcal{R}]\mathbf{a}_1 + [(2n_1 + n_2)/n\mathcal{R}]\mathbf{a}_2$. Its length

$$a = \frac{[3(n_1^2 + n_2^2 + n_1 n_2)]^{1/2}}{n\mathcal{R}} a_0,$$

$$\mathcal{R} = \begin{cases} 3 & \text{if } (n_1 - n_2)/n \in \mathbb{Z}, \\ 1 & \text{otherwise} \end{cases} \tag{1b}$$

is therefore the translational period of the tube.

Clearly, all 2D lattice translations remain symmetries of the tube. Those encountered above produce on the tube pure rotations and pure translations only (making a symmorphic subgroup). The others combine translations and rotations, inevitably yielding helical (screw-axis) symmetry, as a consequence of the underlying hexagonal 2D symmetry. Thus, the $\mathbf{L}^{(1)}$ group of the form $\mathbf{T}_q^r(a)\mathbf{C}_n$ contains the elements $\ell(t, s) = (C_q^r | na/q)^t C_n^s$, where q and r are to be found. At first, it is helpful to note that the action of the screw-axis generator $(C_q^r | na/q)$ manifests itself in a refinement of the elementary cell: within a single translational period there are q/n identical monomers, *i.e.* horizontal slices of the height na/q, each being mapped to the next one by $(C_q^r | na/q)$. Since in the slice there are exactly n 2D lattice cells, the tube cell consists of q 2D cells. On the other hand, the tube cell being on a 2D lattice, the rectangle over $\mathbf{c}/n$ and $\mathbf{a}$ contains

$$q = 2 \frac{n_1^2 + n_1 n_2 + n_2^2}{n\mathcal{R}} \tag{1c}$$

2D lattice cells. Finally, we use the fact that each translation of a 2D lattice uniquely determines an element $\ell(t, s)$: while on the tube the elements $\ell(t, s)$ and $\ell(t, s + n)$ are equal, on the unfolded 2D lattice they correspond to vectors differing by $\mathbf{c}$. Therefore, the whole 2D lattice is generated by elements corresponding to $\ell(t, s)$ ($t, s = 0, \pm 1, \ldots$) and for some particular t and s the lattice basis $\mathbf{a}_1$ and $\mathbf{a}_2$ must be obtained. With the help of elementary number theory (Damnjanović *et al.*, 1999a,b), this requirement gives (the Euler function φ gives the number of coprimes less than or equal to its argument)

$$r = \frac{n_1 + 2n_2 - (n_2/n)^{\varphi(n_1/n)-1} q\mathcal{R}}{n_1 \mathcal{R}},$$

$$p = n\mathcal{R} \frac{[(2n_2 + n_1)/n\mathcal{R}]^{\varphi[(2n_1+n_2)/n\mathcal{R}]-1} q - n_2}{2n_1 + n_2}. \tag{1d}$$
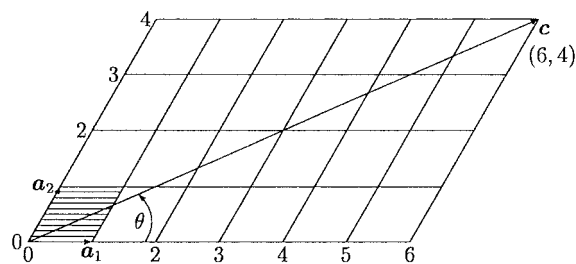
Figure 1
Hexagonal 2D lattice, with basis vectors $\mathbf{a}_1$ and $\mathbf{a}_2$, and shaded elementary cell. The angle between $\mathbf{a}_1$ and the chiral vector $\mathbf{c}$ (determining the tube) is the *chiral angle* θ. The example corresponds to the tube (6,4).

---

[1] The notation used here is a standard crystallographic one specialized for the monoperiodic systems; in the rapidly developing nanotube theory, there are several conventions. *E.g.* in Saito *et al.* (1998), instead of our n, $\mathbf{a}$, a, q, the symbols d, $\vec{T}$, T and N are used, while the quantities multiplied by $\mathcal{R}$ have subscript R.

To comply with the convention providing unique correspondence of the line groups and the helicity parameters r and p, their values should be taken modulo q/n and q, respectively.

This completes the determination of the group $\mathbf{L}^{(1)}$ related to 2D lattice translations only. The other line-group elements depend both on the point symmetries of the 2D layer and on the chiral angle of the considered tube. Combining the structure of the line groups given in Table 1 with the derived form of $\mathbf{L}^{(1)}$, it is easy to see that the candidates to describe symmetry of (hexagonal) tubes are only the line-group families 1, 4, 5, 8 and 13, since the others do not allow a (nontrivial) screw axis. There are two general conclusions further restricting the choice.

First, a horizontal mirror plane and all but the second-order principal-axis rotations of the 2D lattice obviously do not give symmetries of the tube. Consequently, the 2D layers differing only in the horizontal plane are rolled up in tubes with the same symmetry (thus, the neglected deviations of the atoms from the layer plane, which in some cases can destroy the horizontal mirror symmetry, are irrelevant for the final symmetry group; *e.g.* BN tubes). As for the second-order layer axis, it always remains the tube symmetry, becoming the horizontal U axis. Thus, if a layer has such an axis, the tube group contains the fifth family group as a subgroup.

Further, only parallel and perpendicular to the chiral vector vertical mirror planes of the 2D lattice remain symmetries of the tube, becoming horizontal and vertical mirror planes, respectively. Thus, if a 2D lattice possesses vertical mirror planes, the special position of the chiral vectors is singled out, corresponding to the tubes of the enlarged symmetry groups. Following the carbon nanotubes terminology SAI98*b* (Dresselhaus *et al.*, 1998), they will be called *zigzag* and *armchair* tubes, respectively, to differentiate them from the *chiral* tubes with the chiral vector in a general position. With the appropriate choice of $\mathbf{a}_1$ and $\mathbf{a}_2$, these special tubes are $(n, 0)$ and (n, n), respectively, having $q = 2n$, $r = 1$ and $p = n$ by (1) [also, for $(n, 0)$ tubes $\mathcal{R} = 1$, $a = 3^{1/2}a_0$ and, for (n, n) ones, $\mathcal{R} = 3$, $a = a_0$].

Putting together both conclusions, it comes out that if the layer principal axis is of odd order (*i.e.* for the diperiodic group point factors $\mathbf{C}_3$, $\mathbf{S}_6$, $\mathbf{D}_3$, $\mathbf{C}_{3h}$, $\mathbf{C}_{3v}$, $\mathbf{D}_{3d}$ and $\mathbf{D}_{3h}$), the chiral tubes have the first family line-group symmetry

$$\mathbf{L}_\mathcal{C} = \mathbf{T}_q^r(a)\mathbf{C}_n = \mathbf{L}q_p. \tag{2a}$$

When the point symmetry of the layer is one of $\mathbf{C}_{3v}$, $\mathbf{D}_{3d}$ and $\mathbf{D}_{3h}$, the zigzag and armchair tube line groups are from the eighth and fourth families, respectively:

$$\mathbf{L}_\mathcal{Z} = \mathbf{T}_{2n}^1(a)\mathbf{C}_{nv} = \mathbf{L}2n_nmc, \tag{2b}$$

$$\mathbf{L}_\mathcal{A} = \mathbf{T}_{2n}^1(a)\mathbf{C}_{nh} = \mathbf{L}2n_n/m. \tag{2c}$$

In the other case, if there is an even-order principal axis of the layer (the diperiodic group point factor is one of $\mathbf{C}_6$, $\mathbf{D}_6$, $\mathbf{C}_{6v}$, $\mathbf{C}_{6h}$ and $\mathbf{D}_{6h}$), the chiral tube symmetry groups are from the fifth family. Since the presence of the U axis allows only coincidental appearance of vertical and horizontal mirror planes, both zigzag and armchair tubes (for the layer-point

symmetries described by $\mathbf{C}_{6v}$ or $\mathbf{D}_{6h}$) have a symmetry group of the 13th family:

$$\mathbf{L}_\mathcal{C} = \mathbf{T}_q^r(a)\mathbf{D}_n = \mathbf{L}q_p22, \tag{3a}$$

$$\mathbf{L}_{\mathcal{Z},\mathcal{A}} = \mathbf{T}_{2n}^1(a)\mathbf{D}_{nh} = \mathbf{L}2n_n/mcm. \tag{3b}$$

4. Symmetry groups of reported tubes

It remains to obtain the symmetry groups of various tubes analyzing their specific layers separately. This will be performed in the order of increasing symmetry and system complexity. The quantities related to the chiral, zigzag and armchair tubes will be indexed by $\mathcal{C}$, $\mathcal{Z}$ and $\mathcal{A}$. The orbit types of the atoms are denoted according to Milošević & Damnjanović (1993) and Milošević *et al.* (1996, 1997) in the coordinate system with the z axis being the tube axis and the x axis through the lattice point $(0, 0)$ in the figures. The diperiodic groups are denoted according to Wood (1964), Litvin & Wike (1991) and Milošević *et al.* (1998).

4.1. BN and GaN tubes

The layer lattice (Fig. 2) diperiodic group is $\mathbf{Dg}78 = p\bar{6}m2$. Its point factor $\mathbf{D}_{3h}$ has vertical mirror planes and third-order principal axis. Thus, the symmetry groups of the synthesized BN (Blase *et al.*, 1994; Rubio *et al.*, 1994; Loiseau *et al.*, 1996; Weng-Sieh *et al.*, 1995) and only proposed GaN (Lee *et al.*,
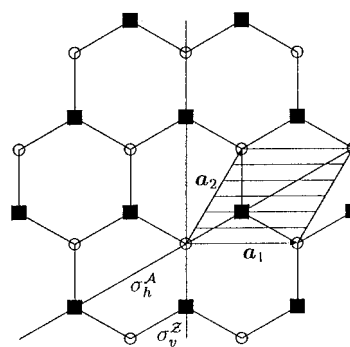
Figure 2
Hexagonal 2D lattice of BN and GaN (B, Ga = circles, N = black square, with mirror planes $\sigma_{v,h}^{\mathcal{Z}/\mathcal{A}}$ remaining in zigzag and armchair tubes; $a_0 \approx 2.5$ Å for BN and $a_0 \approx 3$ Å for GaN).
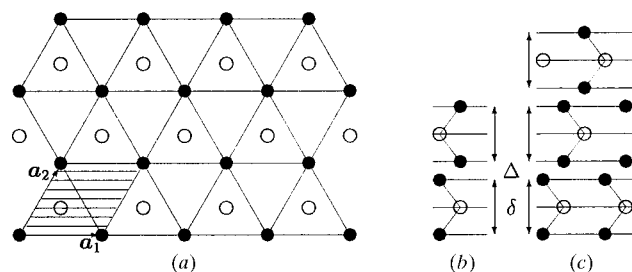
Figure 3
MS$_2$ layers. (*a*) Perpendicular projection of the monolayer S–M–S (white circle = M, black circle = S; $a_0 \approx 3$ Å); the elementary cell of the monolayer (shaded) contains two overlapping sulfur and one transition-metal atom. (*b*) and (*c*) Cross section of $2Hb$ and $3R$ polytypes.

Table 1
Line groups.

For each family of the line groups, the International symbol, different factorizations, generators, the subgroup $\mathbf{L}^{(1)}$ and the isogonal point group $\mathbf{P}_I$ are given. Here, $\mathbf{T}_{cd}$ and U' are the glide plane and horizontal axis bisecting the vertical mirror planes of $\mathbf{P}$. For the groups of families 1 and 5, q is a multiple of n [instead of r, the helicity in the International symbol is given by its modular inverse $p = n(r^{-1} (\mathrm{mod}\, q/n))$].

	International symbol		Factorizations	Generators	$\mathbf{L}^{(1)}$	$\mathbf{P}_I$
	n even	*n* odd				
1	$\mathbf{L}q_p$		$\mathbf{T}_q^r \otimes \mathbf{C}_n$	z_q^r, C_n	$\mathbf{T}_q^r \otimes \mathbf{C}_n$	$\mathbf{C}_q$
2	$\mathbf{L}(\overline{2n})$	$\mathbf{L}\bar{n}$	$\mathbf{T} \wedge \mathbf{S}_{2n}$	$z_0, C_{2n}\sigma_h$	$\mathbf{T} \otimes \mathbf{C}_n$	$\mathbf{S}_{2n}$
3	$\mathbf{L}(\overline{2n})$	$\mathbf{L}n/m$	$\mathbf{T} \wedge \mathbf{C}_{nh}$	z_0, C_n, σ_h	$\mathbf{T} \otimes \mathbf{C}_n$	$\mathbf{C}_{nh}$
4	$\mathbf{L}(2n)_n/m$		$\mathbf{T}_{2n}^1\mathbf{C}_{nh} = \mathbf{T}_{2n}^1\mathbf{S}_{2n}$	z_{2n}^1, C_n, σ_h	$\mathbf{T}_{2n}^1\mathbf{C}_n$	$\mathbf{C}_{2nh}$
5	$\mathbf{L}q_p22$	$\mathbf{L}q_p2$	$\mathbf{T}_q^r \wedge \mathbf{D}_n$	z_q^r, C_n, U	$\mathbf{T}_q^r \otimes \mathbf{C}_n$	$\mathbf{D}_q$
6	$\mathbf{L}nmm$	$\mathbf{L}nm$	$\mathbf{T} \otimes \mathbf{C}_{nv} = \mathbf{C}_{nv} \wedge \mathbf{T}_{cd}$	z_0, C_n, σ_v	$\mathbf{T} \otimes \mathbf{C}_n$	$\mathbf{C}_{nv}$
7	$\mathbf{L}ncc$	$\mathbf{L}nc$	$\mathbf{C}_n \wedge \mathbf{T}_c$	z_v, C_n	$\mathbf{T} \otimes \mathbf{C}_n$	$\mathbf{C}_{nv}$
8	$\mathbf{L}(2n)_nmc$		$\mathbf{C}_{nv} \wedge \mathbf{T}_{2n}^1 = \mathbf{C}_{nv} \wedge \mathbf{T}_{cd}$	z_{2n}^1, C_n, σ_v	$\mathbf{T}_{2n}^1 \otimes \mathbf{C}_n$	$\mathbf{C}_{2nv}$
9	$\mathbf{L}(\overline{2n})2m$	$\mathbf{L}\bar{n}m$	$\mathbf{T} \wedge \mathbf{D}_{nd} = \mathbf{T}_c \wedge \mathbf{D}_{nd}$	z_0, C_n, U', σ_v	$\mathbf{T} \otimes \mathbf{C}_n$	$\mathbf{D}_{nd}$
10	$\mathbf{L}(\overline{2n})2c$	$\mathbf{L}\bar{n}c$	$\mathbf{T}_c\mathbf{S}_{2n} = \mathbf{T}_{cd}\mathbf{D}_n$	z_v, C_n, U'	$\mathbf{T} \otimes \mathbf{C}_n$	$\mathbf{D}_{nd}$
11	$\mathbf{L}n/mmm$	$\mathbf{L}(\overline{2n})2m$	$\mathbf{T} \wedge \mathbf{D}_{nh} = \mathbf{T}_c\mathbf{D}_{nh}$	z_0, C_n, U, σ_v	$\mathbf{T} \otimes \mathbf{C}_n$	$\mathbf{D}_{nh}$
12	$\mathbf{L}n/mcc$	$\mathbf{L}(\overline{2n})2c$	$\mathbf{T}_c\mathbf{C}_{nh} = \mathbf{T}_c\mathbf{D}_n$	z_v, C_n, U	$\mathbf{T} \otimes \mathbf{C}_n$	$\mathbf{D}_{nh}$
13	$\mathbf{L}(2n)_n/mcm$		$\mathbf{T}_{2n}^1\mathbf{D}_{nh} = \mathbf{T}_{2n}^1\mathbf{D}_{nd}$ $= \mathbf{T}_c\mathbf{D}_{nh} = \mathbf{T}_c\mathbf{D}_{nd}$	$z_{2n}^1, C_n, U, \sigma_v$	$\mathbf{T}_{2n}^1 \otimes \mathbf{C}_n$	$\mathbf{D}_{2nh}$

1999) tubes are (2). The tubes are two orbit systems, generated by the transversal being the group (2a) from the pair of atoms of B (or Ga) and N. Both orbits are of the types a_1, b_1 and d_1, with corresponding stabilizers $\mathbf{C}_1$, $\mathbf{C}_{1v}$ and $\mathbf{C}_{1h}$, respectively, for chiral, zigzag and armchair tubes.

4.2. Transition-metal dichalcogenide tubes

Here we refer to two compounds, MoS_2 and WS_2, having the same structure both in the layer and in the tubular forms. The tubes consist (Wilson & Yoffe, 1969; Tenne *et al.*, 1992) of two or three monolayers M–S–M (M = Mo, W), each of them being the pair of the parallel sulfur planes at a distance $\delta \approx 6$ Å, bisected by the transition-metal plane (Fig. 3). The sulfur atoms of the different planes are one above another, while the metal atoms are between the centers of the sulfur triangles [*i.e.* translated by $(\mathbf{a}_1 + \mathbf{a}_2)/3$]. Thus the layer elementary cell contains two S (one above another) and one transition-metal atoms.

Both WS_2 and MoS_2 crystallize in the following two forms differing in the layer repeated along the c direction. The layer of the hexagonal $2Hb$ polytype contains two monolayers, the second one being rotated by $\pi/3$ (around the perpendicular axis through S) and then translated for $(\mathbf{a}_1 + \mathbf{a}_2)/3$, resulting in the interchange of the S- and M-atom positions. A single layer of the $3R$ polytype consists of three monolayers: with respect to the first one, the second is translated by $(\mathbf{a}_1 + \mathbf{a}_2)/3$ (S atoms are moved above M atoms of the first monolayer), and the third by $2(\mathbf{a}_1 + \mathbf{a}_2)/3$ (its M atoms get above the S atoms of the first layer). In both cases, the distance between the monolayers (Wilson & Yoffe, 1969) is $\Delta \approx 2$ Å. The tubes with the walls of both polytype layers are observed (Tenne *et al.*, 1998; Remškar, Škraba, Ballif, Sanjinés & Lévy, 1999): the nanotubes (diameters less than 0.1 µm) grow in the hexagonal $2Hb$ polytype, and the microtubes (diameters greater than

2 µm) prefer the rhombohedral $3R$ polytype (Remškar, Škraba, Sanjinés & Lévy, 1999).

Despite the difference in the space groups of crystalline polytypes, namely $P6_3/mmc$ for $2Hb$ and $R3m$ for $3R$, they have the same diperiodic group $\mathbf{Dg}69 = p3m1$ (point factor $\mathbf{C}_{3v}$) implying that the resulting tubes have the same symmetry. In fact, these groups coincide with that of the monolayered tubes (not observed yet) of the same chirality, since the monolayer group $\mathbf{Dg}78 = p\bar{6}m2$, with point factor $\mathbf{D}_{3h}$, differs only in an additional horizontal plane. The odd order of the principal axis of all these layers means that, depending on the chirality, the tube line group is one of (2). While the monolayered tubes have 3 orbits (two S and one M), the single-layered $2Hb$ and $3R$ tubes consist of 6 and 9 orbits, respectively, being of the same type as for the BN tubes.

4.3. Carbon tubes

These are the most extensively studied tubes (Iijima, 1991) and have a 2D layer of graphite honeycomb lattice (Fig. 4). Its symmetry is $\mathbf{Dg}80 = p\frac{6}{m}\frac{2}{m}\frac{2}{m}$, with the point factor $\mathbf{D}_{6h}$. The layer's second-order vertical axes (two non-equivalent types) lead to the tube line groups (3). Each carbon single-wall nanotube is a mono orbit system, with the orbits being of types a_1 (chiral), b_1 (zigzag) and d_1 (armchair), with respective stabilizers $\mathbf{C}_1$, $\mathbf{C}_{1v}$ and $\mathbf{C}_{1h}$; the transversal is the chiral group (3a) for all chiralities.

4.4. BC₃ tubes

The BC_3 layer (Fig. 5) symmetry group is $\mathbf{Dg}80$, as for graphite, but with approximately doubled lattice vectors used to define the chiral vector [thus a_0 in (1b) is doubled, resulting in the doubled translational period]. Consequently, the symmetry groups of BC_3 tubes (Miyamoto, Rubio, Louie & Cohen, 1994) are the same as for the carbon nanotubes (3).
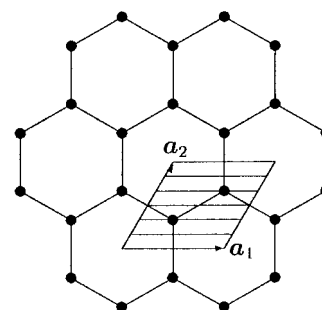
Figure 4
Honeycomb graphite lattice ($a_0 = 2.46$ Å).

Now, there are three C orbits and one B orbit of a_1 type with trivial stabilizer, in the chiral case. In the achiral cases, besides one C orbit of the type a_1 [trivial stabilizer and the transversal $(3b)$], there is one C and one B orbit of the type b_1 (stabilizer $\mathbf{C}_{1v}$) in the zigzag case or of the type d_1 (stabilizer $\mathbf{C}_{1h}$) in the armchair case; transversal of both b_1 and d_1 orbits is the group $(3a)$.

4.5. BC$_2$N tubes (type I)

There are several 2D lattices corresponding to this chemical structure. Here we consider two configurations, the most stable ones (Miyamoto, Rubio, Cohen & Louie, 1994; Weng-Sieh *et al.*, 1995) having quite different geometry and resulting symmetry. Though the symmetry of these layers is not hexagonal, the previous results can be used owing to the possibility of choosing suitable lattice vectors (making an angle of $\pi/3$, with convenient length ratio).

The type I tube (Fig. 6) has approximately doubled lattice vectors with respect to graphite but, contrary to the latter, the actual diperiodic group $\mathbf{Dg}37 = p\frac{2}{m}\frac{2}{m}\frac{2}{m}$ retains only $C_6^3 = C_2$ rotation and two vertical mirror planes, leaving the point factor $\mathbf{D}_{2h}$. Therefore, although the symmetry groups of the tubes are given by (3), as for the carbon tubes, the inequivalent tubes are between the chiral directions $(n, 0)$ and $(-n, 2n)$ (with chiral angles between 0 and $\pi/2$), and zigzag and armchair cases refer only to such cases, respectively [all other chiral vectors, (n, n) inclusive, give chiral tubes]. A chiral tube is built of two C, one B and one N orbits of the type a_1 [trivial stabilizer and whole group $(3a)$ as the transversal]; in the achiral cases, C orbits are joined in the single general C orbit [a_1 with trivial stabilizer and the transversal being the group $(3b)$], while B and N each form the orbits of the b_1 (zigzag), *i.e.* d_1 (armchair) type. The corresponding stabilizers are $\mathbf{C}_{1v}$ and $\mathbf{C}_{1h}$, respectively, while in both cases the transversal is the group $(3a)$.

4.6. BC$_2$N tubes (type II)

The second type of BC$_2$N tube has the underlying lattice presented in Fig. 7. The elementary cell is doubled with respect to the hexagonal lattice over $\mathbf{a}_1$ and $\mathbf{a}_2$, since the periods are $\mathbf{a}_1$ and $\mathbf{A}_2 = 2\mathbf{a}_2$. In the layer's diperiodic group
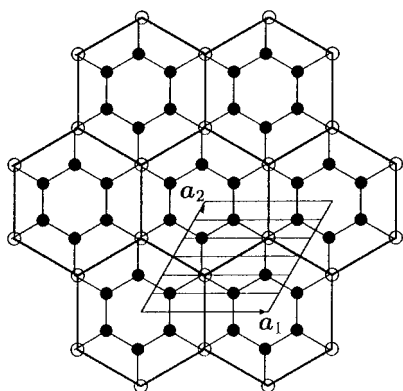
$\mathbf{Dg}24 = pmm2$, there is only a trivial principal axis, but the vertical mirror plane of the point factor $\mathbf{D}_{1h}$ enables one to consider as inequivalent tubes (optical isomers are assumed equivalent) only those with the chiral angles between 0 and $\pi/2$. Again, the tubes with $\theta = 0$ are called zigzag, those with $\theta = \pi/2$ armchair and the other ones chiral. Since the chiral vector of (n_1, n_2) corresponds to an $(n_1, 2n_2)$ hexagonal tube, the latter will be used to derive the wanted symmetry group: only those rototranslations of this auxiliary tube that correspond to the hexagonal lattice translations with even $\mathbf{a}_2$ (*i.e.* integer $\mathbf{A}_2$) component are the symmetries of the studied BC$_2$N tube. Such transformations make on the tube a halving subgroup of (2) parametrized by (1) with $2n_2$ used instead of n_2. Since no U axis appears, this subgroup is the symmetry group which is looked for:

$$\mathbf{L}_\mathcal{C} = \mathbf{T}_Q^R(A)\mathbf{C}_N = \mathbf{L}Q_P. \qquad (4a)$$

The values of the group parameters Q, R, N, P and A, derived utilizing the direct product structure (Damnjanović & Vujičić, 1981) of the group (2), are given in Table 2.

For both zigzag $(n, 0)$ and armchair $(-n, n)$ tubes, $\tilde{n}_1 = 1$, making relevant the first row of the table. The obtained value $q = 2n$, *i.e.* $Q = N$, means that the achiral symmetry groups are symmorphic, manifesting rectangular layer symmetry. When completed by σ_v, *i.e.* σ_h, they become the line groups of the third and sixth families, respectively:

$$\mathbf{L}_\mathcal{Z} = \mathbf{T}(3^{1/2}a_0)\mathbf{C}_{nv} = \mathbf{L}nmm, \, \mathbf{L}nm, \qquad (4b)$$

$$\mathbf{L}_\mathcal{A} = \mathbf{T}(a_0)\mathbf{C}_{nh} = \mathbf{L}(\overline{2n}), \, \mathbf{L}n/m. \qquad (4c)$$

A chiral tube is built of two C, one B and one N orbits of the type a_1 [trivial stabilizer and group $(2a)$ being the transversal]. In the zigzag case, two C orbits are both of b_1 type for n odd, while for even n one of them is of b_1 and the other one of c_1 type (for both types the stabilizer $\mathbf{C}_{1v}$ with different mirror plane); B atoms form a b_1 type orbit, while the orbit of N atoms is b_1 when n is odd and c_1 otherwise. In the armchair case, two orbits of C atoms are a_2 and b_1 with stabilizers $\{e, (\sigma_h|1)\}$ and $\mathbf{C}_{1h}$; N and B atoms form a_2 and b_1 orbits, respectively. For all the achiral orbits, the transversal is index-2 subgroup $\mathbf{TC}_n$.
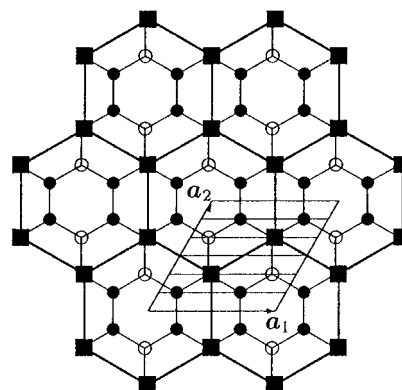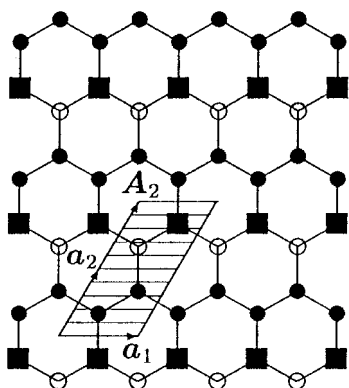

Figure 5
Lattice of BC$_3$ layer (B = white circle, C = black circle, $a_0 \approx 5.14$ Å).

Figure 6
Lattice of BC$_2$N type I layer (B = white circle, C = black circle, N = black square, $a_0 \approx 5$ Å).

5. Concluding remarks

All the geometrical symmetries of the nanotubes reported in the literature are found. In addition to the rotations, translations and screw axes, some of the known single-wall tubes possess horizontal rotational axes. Also, zigzag and armchair tubes have vertical and horizontal mirror planes, respectively. If the 2D lattice of the unrolled tube has even-order principal axis, the horizontal U axis emerges as tube symmetry and the resulting line group for the zigzag and armchair cases is the same. Combined with special type screw axes, the mirror planes of achiral tubes give vertical glide planes $\mathbf{T}_c$ and rotoreflection axes $\mathbf{S}_{2n}$, respectively. The parameters q and r of the helical group (screw axis) are found in the closed form. Since $2\pi/q$ is the angle of the minimal rotation (combined with the fractional translation) performed by the symmetry group, the order of the principal axis of the isogonal group is q and it is always even (Damnjanović et al., 1999a,b). Moreover, q is the number of 2D lattice cells in the elementary translational cell of the tube. The variety of the symmetry groups obtained for each type of tube shows that the properties of the nanotubes may vary greatly, depending on their chiralities.

There are many physical properties based on symmetry and the presented classification of nanotubes according to their symmetry can be widely exploited. At first, the symmetry can be used to find good quantum numbers and related selection rules. These are related to the irreducible representations of the found group. Besides the z component k of quasi-momentum, in the literature is used also the z component m of angular momentum and helical momenta, $\tilde{k}$ and $\tilde{m}$. In fact, the latter is the momentum canonically conjugated to the helix generated by the screw-axis generator $(C_q^r|na/q)$, obviously including a part of m, while the remaining part is $\tilde{m}$. It should be emphasized that m is not a conserved quantum number, since it originates from the isogonal point group, which in nonsymmorphic cases is not symmetry of the system. Selection rules can be easily found with these conserved quantum numbers.

The orbit types given for each of the tubes characterize the system. Besides the possibility to define the system by these data, they are relevant in all quantum-mechanical calculations

Table 2
The parameters Q, R, N, P and A of the line group $\mathbf{L}_{\mathcal{C}}$ of a type II BC$_2$N tube (n_1, n_2).

q, r, n, p and a are given by (1) for the hexagonal tube $(n_1, 2n_2)$. The values depend on the parity of the auxiliary parameters $\tilde{n}_1 = n_1/\mathrm{GCD}(n_1, n_2)$, and for even $\tilde{n}_1$ of $x = (1 + r\mathcal{R} + \tilde{n}_1)/2$ and $y = (pr - n)/q$.

Q	R	N	P	A	$\tilde{n}_1$	x	y
$q/2$	$r\,(\mathrm{mod}\,q/(2n))$	n	$p\,(\mathrm{mod}\,q/2)$	a	Odd	–	–
q	r	$n/2$	$p/2$	$2a$	Even	Even	Even
q	r	$n/2$	$(p+q)/2$	$2a$	Even	Even	Odd
q	$(r+q/n)\,(\mathrm{mod}\,q)$	$n/2$	$(p+q)/2$	$2a$	Even	Odd	Even
q	$(r+q/n)\,(\mathrm{mod}\,q)$	$n/2$	$p/2$	$2a$	Even	Odd	Odd

performed in the space induced over the atoms. Here come e.g. the tight-binding approach to electronic bands (Hamada et al., 1992; White et al., 1993; Jishi et al., 1995; Saito et al., 1998; Dresselhaus et al., 1998; Reich & Thomsen, 2000), vibrational (Saito et al., 1998; Milošević & Damnjanović, 1993; Milošević et al., 1996, 1997; Dresselhaus et al., 1998) and spin wave analysis. In fact, they enable complete classification of the corresponding bands and degeneracies, and maximal possible simplification of the corresponding dispersion relations.

Let us mention again that this method can be easily generalized to the tubes with a non-hexagonal underlying 2D lattice. For example, the results for type II BC$_2$N tubes may be obtained even more easily and in more compact form with parametrization $\mathbf{c} = N_1\mathbf{a}_1 + N_2(\mathbf{a}_2 - \mathbf{a}_1)$ corresponding to rectangular basis $\mathbf{a}_1$, $\mathbf{a}_2 - \mathbf{a}_1$ of a 2D lattice. For clarity, we present only the hexagonal-lattice-based analysis, and it suffices even for BC$_2$N tubes, which are the only reported exception in this sense. The method may also be generalized to study the symmetry of multiwall tubes, along the lines sketched for multiwall carbon tubes (Damnjanović et al., 1999a,b).

References

Blase, X., Rubio, A., Louie, S. G. & Cohen, M. L. (1994). *Europhys. Lett.* **28**, 335–340.

Damnjanović, M., Milošević, I., Vuković, T. & Sredanović, R. (1999a). *J. Phys. A*, **32**, 4097–4104.

Damnjanović, M., Milošević, I., Vuković, T. & Sredanović, R. (1999b). *Phys. Rev. B*, **60**, 2728–2739.

Damnjanović, M. & Vujičić, M. (1981). *J. Phys. A*, **14**, 1055–1063.

Dresselhaus, M., Dresselhaus, G. & Eklund, P. (1998). *Science of Fullerenes and Carbon Nanotubes*. San Diego: Academic Press.

Dresselhaus, M., Dresselhaus, G. & Saito, R. (1992). *Phys. Rev. B*, **45**, 6234–6243.

Hamada, N., Sawada, S. & Oshiyama, A. (1992). *Phys. Rev. Lett.* **68**, 1579–1581.

Iijima, S. (1991). *Nature (London)*, **354**, 56–58.

Janssen, T. (1973). *Crystallographic Groups.* Amsterdam: North-Holland.

Jishi, R. A., Venkataraman, L., Dresselhaus, M. S. & Dresselhaus, G. (1995). *Phys. Rev. B*, **51**, 11176–11179.

Lee, S. M., Lee, Y. H., Hwang, Y. G., Elsner, J., Porezag, D. & Frauenheim, T. (1999). *Phys. Rev. B*, **60**, 7788–7791.

Litvin, D. B. & Wike, T. R. (1991). *Character Tables and Compatibility Relations of the 80 Layer Groups and 17 Plane Groups.* New York: Plenum Press.

Figure 7
Lattice of BC$_2$N type II layer (B = white circle, C = black circle, N = black square; $a_0 \approx 2.5$ Å).

research papers

Loiseau, A., Willaime, F., Demoncy, N., Hug, G. & Pascard, H. (1996). *Phys. Rev. Lett.* **76**, 4737–4740.

Milošević, I., Damnjanović, A. & Damnjanović, M. (1996). *Quantum Mechanical Simulation Methods in Studying Biological Systems*, edited by D. Bicout & M. Field, ch. XIV. Berlin: Springer-Verlag.

Milošević, I. & Damnjanović, M. (1993). *Phys. Rev. B*, **47**, 7805–7818.

Milošević, I., Nikolić, B., Damnjanović, M. & Krčmar, M. (1998). *J. Phys. A*, **31**, 3625–3648.

Milošević, I., Živanović, R. & Damnjanović, M. (1997). *Polymer*, **38**, 4445–4453.

Miyamoto, Y., Rubio, A., Cohen, M. L. & Louie, S. G. (1994). *Phys. Rev. B*, **50**, 4976–4979.

Miyamoto, Y., Rubio, A., Louie, S. G. & Cohen, M. L. (1994). *Phys. Rev. B*, **50**, 18360–18366.

Reich, S. & Thomsen, C. (2000). *Phys. Rev. B*, **62**, 4273–4276.

Remškar, M., Škraba, Z., Ballif, C., Sanjinés, R. & Lévy, F. (1999). *Surf. Sci.* **433–435**, 637–641.

Remškar, M., Škraba, Z., Sanjinés, R. & Lévy, F. (1999). *Appl. Phys. Lett.* **74**, 3633–3635.

Rubio, A. Corkill, J. L. & Cohen, M. L. (1994). *Phys. Rev. B*, **49**, 5081–5084.

Saito, R., Dresselhaus, G. & Dresselhaus, M. (1998). *Physical Properties of Carbon Nanotubes*. London: Imperial College Press.

Tenne, R., Homyonfer, M. & Feldman, Y. (1998). *Chem. Mater.* **10**, 3225–3238.

Tenne, R., Margulis, L., Genut, M. & Holdes, G. (1992). *Nature (London)*, **360**, 444.

Weng-Sieh, Z., Cherrey, K., Chopra, N. G., Blase, X., Miyamoto, Y., Rubio, A., Cohen, M. L., Louie, S. G., Zettl, A. & Gronsky, R. (1995). *Phys. Rev. B*, **51**, 11229–11232.

White, C. T., Robertson, D. H. & Mintmire, J. W. (1993). *Phys. Rev. B*, **47**, 5485–5488.

Wilson, J. A. & Yoffe, A. D. (1969). *Adv. Phys.* **18**, 193–335.

Wood, E. A. (1964). *80 Diperiodic Groups in Three Dimensions*. Bell System Monograph No. 4680.